

A new approach for the limit to tree height using a liquid nanolayer model

Henri Gouin

*University of Aix-Marseille & C.N.R.S. U.M.R. 6181,
Case 322, Av. Escadrille Normandie-Niemen, 13397 Marseille Cedex 20 France*

Published in *Continuum Mechanics and Thermodynamics*.
Accepted after revision on 15 August 2008, in Vol. **20**, 5 (2008).

On line first: 10 September 2008

"The original publication is available at www.springerlink.com"

DOI: 10.1007/s00161-008-0084-y

Abstract

Liquids in contact with solids are submitted to intermolecular forces inferring density gradients at the walls. The van der Waals forces make liquid heterogeneous, the stress tensor is not any more spherical as in homogeneous bulks and it is possible to obtain stable thin liquid films wetting vertical walls up to altitudes that incompressible fluid models are not forecasting. Application to micro tubes of xylem enables to understand why the ascent of sap is possible for very high trees like sequoias or giant eucalyptus.

Key words: nanofilms, inhomogeneous liquids, van der Waals forces, ascent of sap, high trees.

PACS: 68.65.k, 82.45.Mp, 87.10.+e, 87.15.Kg, 87.15.La

1 Introduction

In *Amazing numbers in biology*, Flindt reports an eucalyptus of 128 meters and a giant sequoia of 135 meters [1]. However, biophysical determination of maximum size to which trees can grow is not well understood [2]. A main problem with the understanding of tall trees is why the sap is able to reach so high levels.

Email address: henri.gouin@univ-cezanne.fr (Henri Gouin).

Xylem tube diameters range between 50 and 400 μm ; the crude sap contains diluted salts but its physical properties are roughly those of water. Consequently, hydrodynamic, capillarity and osmotic pressure create a sap ascent of only few tens of meters [3]. To explain the sap ascent phenomenon, Dixon and Joly proposed in 1894 a cohesion-tension model [4], followed by a quantitative attempt by van der Honert in 1948 [5]: liquids may be subjected to tensions generating negative pressures compensating gravity effects. Nevertheless, thermodynamic states are strongly metastable and can generate cavitation causing embolisms in xylem tubes made of dead cells [6].

As pointed out in Ref. [7], a turning-point in the pro and con debate on the sap ascent was the experiment of Preston in 1952 who demonstrated that tall trees survived overlapping double saw-cuts made through the cross-sectional area of the trunk to sever all xylem elements [8]. This result, confirmed later by several authors (e.g. Mackey & Weatherley in 1973 [9]; Eisenhut, in 1988 [10]; Benkert *et al* in 1991 [11]), was obviously not in agreement with the cohesion-tension theory. Using a xylem pressure probe, Balling and Zimmermann showed up that, in many circumstances, this apparatus does not measure any water tension [12]. Since these experiments, Zimmermann *et al* questioned the cohesion-tension theory in Ref. [13]: xylem tension exceeding 0.6 Mpa was not observed and in normal state most vessels were found to be embolized at a level corresponding to sixty meter high [14]¹; consequently trees growing taller than a few tens of meter range are not foreseeable. Recently in their review article Zimmermann *et al* demonstrate that the present interpretation of the pressure bomb data is based on a misconception and that negative xylem pressure values of several megapascals do not exist since xylem sap composition, the features of the xylem wall and the hydraulic coupling of the xylem with the tissue prevent the development of stable tensions larger than about 1 MPa. Moreover, gas-vapor transportation in xylem tubes was found at the top of height trees [7].

In this paper, our ambition is to present an understanding of the ascent of sap in very high trees, different from the cohesion-tension theory: at a higher

¹ It is interesting to remark that xylem tube diameters range between 50 and 400 μm and the crude sap is a liquid bulk with a superficial tension σ lower than the superficial tension of pure water which is 72.5 cgs at 20° Celsius. Let us consider a microscopic gaz-vapor bubble inside the crude sap with a diameter $2R$ smaller than xylem tube diameters. The difference between the gaz-vapor pressure and the liquid sap pressure can be expressed by the Laplace formula: $P_v - P_l = 2\sigma/R$. The vapor-gas pressure is positive and omitted with respect to $|P_l|$; consequently unstable bubbles appear when $R \geq -2\sigma/P_l$. For a negative pressure $P_l = -0.6$ MPa in the sap as pointed out by experiments, we obtain $R \geq 0.24 \mu m$. Due to the diameter range of xylem tubes and the diameter range of bubbles, the Laplace formula is valid at equilibrium for such bubble sizes [15]; dynamical bubbles appear spontaneously from germs naturally included in the liquid when the tubes are filled with the crude sap and cavitation makes the tubes embolized.

level than a few tens of meters - corresponding to the pulling of water by hydrodynamic, capillary and osmotic pressure - we assume that tubes may be embolized. In addition, we assume also that a thin liquid film - with a thickness of a few nanometers [16,17,18] - wets xylem walls up to the top of the tree. At this scale, long range molecular forces stratify liquids [19] and the ratio between tube diameter and sap film thickness allows us to consider tube walls as *plane surfaces*; consequently the problem of sap ascent in vertical tubes is similar to the rise of a liquid film damping a vertical plane wall.

The sap motion in xylem tube can be suitably explained by the transpiration through micropores located in tree leaves [3,7]: evaporation changes the liquid layer thickness implying driving of sap as explained in Ref. [20].

Consequently, this paper aims to prove, in non-evaporating case, the existence at equilibrium of thin films of water wetting vertical walls up to a same order of altitude than the height of very tall trees.

The recent development of experimental technics allows us to observe physical phenomena at length scales of a few nanometers. This nanophysics reveals behaviors often surprising and basically different from those that can be observed at a microscopic scale [21].

At the end of the nineteenth century, the fluid inhomogeneity in liquid-vapor interfaces was taken into account by considering a volume energy depending on space density derivative [22,23]. In the first part of the twentieth century, Rocard obtained a thermodynamical justification of the model by an original step in kinetic theory of gases [24]. This van der Waals square-gradient functional is unable to model repulsive force contributions and misses the dominant damped oscillatory packing structure of liquid layers near a substrate wall [25,26]. Furthermore, the decay lengths are only correct close to the liquid-vapor critical point where the damped oscillatory structure is subdominant [27,28]. Recently, in mean field theory, weighted density-functional has been used to explicitly demonstrate the dominance of this structural contribution in van der Waals thin films and to take into account long-wavelength capillary-wave fluctuations as in papers that renormalize the square-gradient functional to include capillary wave fluctuations [29,30]. In contrast, fluctuations strongly damp oscillatory structure and it is mainly for this reason that van der Waals' original prediction of a *hyperbolic tangent* is so close to simulations and experiments [31].

To get an analytic expression in density-functional theory for a thin liquid film near a solid wall, we add a liquid density-functional at the solid surface to the square-gradient functional representing closely liquid-vapor interface free energy. This kind of functional is well-known in the literature, as the general background studied by Nakanishi and Fisher [32]. It was used by Cahn in a phenomenological form, in a well-known paper studying wetting near a critical point [33]. An asymptotic expression is obtained in [34] with an approximation of hard sphere molecules and London potentials for liquid-liquid and solid-liquid interactions: by using London or Lennard-Jones potentials, we

took into account the power-law behavior which is dominant in a thin liquid film in contact with a solid. In this paper, the effects of the vapor bulk bordering the liquid film are simply expressed with an other density-functional of energy located on a mathematical surface as a dividing-like surface for liquid-vapor interfaces of a few Angström thickness.

With this functional, we obtain the equations of equilibrium [35] and boundary conditions [36] for a thin vertical liquid film damping a vertical solid wall and we can compute the liquid layer thickness as a function of the film level. Moreover, the normal stress vector acting on the wall is constant through the liquid layer and corresponds to the gas-vapor bulk pressure which is currently the atmospheric pressure; no negative pressure appears in the liquid layer.

As in [37], several methods can be used to study the stability of a thin liquid film in equilibrium. In our case, the *disjoining pressure* of a thin liquid layers is a well adapted tool for very thin films. By using Gibbs free energy per unit area for the liquid layer as a function of the thickness, we are able to obtain the minimal thickness for which a stable wetting film damps a solid wall. The minimal thickness is associated with the *pancake layer* when the film is bordering the dry solid wall [16,38,39] and corresponds to a maximal altitude. Numerical calculations associated with physical values for water yield the maximal film altitude for a silicon wall and a less hydrophile material. In the two cases, we obtain an approximative maximum level corresponding to a good height order for the tallest trees.

2 Definition and well-known results of the disjoining pressure

Without redoing or demonstrating the main results of Derjaguin *et al* [16] related to thin liquid films and the well-known *disjoining pressure*, we enumerate the properties we apply in the problem of rise of a liquid on a vertical wall.

In this paper, we consider fluids and solids *at a given temperature* θ . The film is thin enough such that the gravity effect is neglected across the liquid layer. The hydrostatic pressure in a thin liquid layer included between a solid wall and a vapor bulk differs from the pressure in the contiguous liquid phase. At equilibrium, the additional interlayer pressure is called the *disjoining pressure*. Clearly, a disjoining pressure could be measured by applying an external pressure to keep the complete layer in equilibrium. The measure of a disjoining pressure is either the additional pressure on the surface or the drop in the pressure within the *mother bulks* which produce the layer. In both cases, the forces arising during the thinning of a film of uniform thickness h produce the disjoining pressure $\Pi(h)$ of the liquid layer with the surrounding phases; the disjoining pressure is equal to the difference between the pressure P_{v_b} on the interfacial surface (which is the pressure of the *vapor mother bulk* of density

ρ_{v_b}) and the pressure P_b in the *liquid mother bulk* (density ρ_b) from which the liquid layer extends (this is the reason for which Derjaguin used the term *mother bulk* [16], page 32) :

$$\Pi(h) = P_{v_b} - P_b. \quad (1)$$

The most classical apparatus to measure the disjoining pressure is due to Sheludko [40] and is described on Fig. (1). Let us consider the Gibbs free

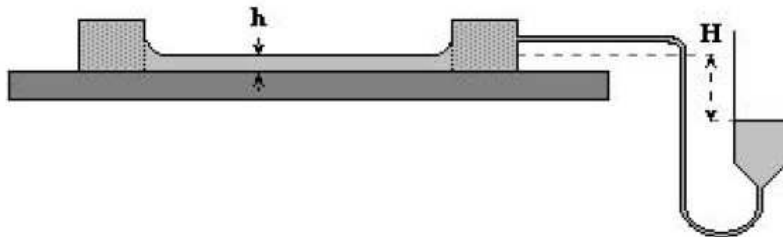


Fig. 1. Diagram of the technique for determining the disjoining pressure isotherms of wetting films on a solid substrate: a circular wetting film is formed on a flat substrate to which a microporous filter is clamped. A pipe connects the filter filled with the liquid to a reservoir containing the liquid mother bulk that can be moved by a micrometric device. As we will see in section 5, the thickness h of the film depends on H in a convenient domain of H values where the wetting film is stable. The disjoining pressure is equal to $\Pi = (\rho_b - \rho_{v_b}) g H$, where g is the acceleration of gravity (From Ref. [16], page 332).

energy of the liquid layer (thermodynamic potential). As proved by Derjaguin *et al* in Ref. ([16], Chapter 2), the Gibbs free energy per unit area G can be expressed as a function of h :

$$\frac{\partial G(h)}{\partial h} = -\Pi(h). \quad (2)$$

Eq. (2) can be integrated as :

$$G(h) = \int_h^{+\infty} \Pi(h) dh \quad (3)$$

where $h = 0$ is associated with the dry wall in contact with the vapor bulk and $h = +\infty$ is associated with a wall in contact with liquid bulk when the value of G is 0.

An important property related to the problem of wetting is associated with the well-known spreading coefficient :

$$S = \gamma_{SV} - \gamma_{SL} - \gamma_{LV},$$

where $\gamma_{SV}, \gamma_{SL}, \gamma_{LV}$ are respectively the solid-vapor, solid-liquid and liquid-vapor free energies per unit area of interfaces. The energy of the liquid layer

per unit area can be written as :

$$E = \gamma_{SL} + \gamma_{LV} + G(h).$$

When $h = 0$, we obtain the energy γ_{SV} of the dry solid wall; when $h = +\infty$, we obtain $\gamma_{SL} + \gamma_{LV}$. In complete wetting of a liquid on a solid wall, the spreading coefficient is positive and the Gibbs free energy G looks like in Fig. 2.

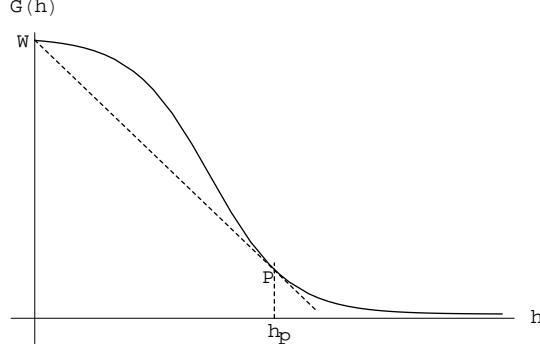


Fig. 2. The construction of the tangent to curve $G(h)$ from point W of coordinates $(0, G(0))$ involves point P ; point W is associated with a high-energy surface of the dry wall and point P is associated with the pancake thickness h_p where the film coexists with the dry wall; it is the smallest stable thickness for the liquid layer.

The conditions of stability of a thin liquid layer essentially depend on phases between which the film is sandwiched. In case of a single film in equilibrium with the vapor and a solid substrate, the stability condition is :

$$\frac{\partial \Pi(h)}{\partial h} < 0 \quad \Leftrightarrow \quad \frac{\partial^2 G(h)}{\partial h^2} > 0. \quad (4)$$

The coexistence of two film segments with different thicknesses is a phenomenon which can be interpreted with the equality of chemical potential and superficial tension of the two films. A spectacular case corresponds to the coexistence of a liquid film of thickness h_p and the dry solid wall associated with $h = 0$. The film is the so-called *pancake layer* corresponding to the condition :

$$G(0) = G(h_p) + h_p \Pi(h_p). \quad (5)$$

Eq. (5) expresses that the value of the Legendre transformation of $G(h)$ at h_p is equal to $G(0)$. Liquid films of thickness $h > h_p$ are stable and liquid films of thickness $h < h_p$ are metastable or unstable.

3 The study of inhomogeneous fluids by using a square-gradient approximation and surface-density functionals at bordering walls

The modern understanding of liquid-vapor interfaces begins with papers of van der Waals and the square-gradient approximation for the free energy of

inhomogeneous fluids. In current approaches, it is possible to give formal exact expressions of the free energy in terms of pair-distribution function and the direct correlation function [41]. In practice, these complex expressions must be approximated to lead to a compromise between accuracy and simplicity. When we are confronted with such complications, the primitive mean-field models are generally inadequate and the obtained qualitative picture is no more sufficient. The main alternatives are density-functional theories which are a lot simpler than the Ornstein-Zernike equation in statistical mechanics since the local density is a functional at each point of the fluid [27,31]. We use this rough approximation enabling us to compute analytically the density profiles of simple fluids. Nevertheless, we take into account surface effects and repulsive forces by adding density-functionals at boundary surfaces. The density-functional of the inhomogeneous fluid in a domain O of boundary ∂O is taken in the form :

$$F = \int \int \int_O \varepsilon \, dv + \int \int_{\partial O} \varpi \, ds. \quad (6)$$

The first integral is associated with a square-gradient approximation when we introduce a specific free energy of the fluid at a given temperature θ ,

$$\varepsilon = \varepsilon(\rho, \beta)$$

as a function of density ρ and $\beta = (\text{grad } \rho)^2$. Specific free energy ε characterizes together the fluid properties of *compressibility* and *molecular capillarity* of liquid-vapor interfaces. In accordance with gas kinetic theory,

$$\rho \varepsilon = \rho \alpha(\rho) + \frac{\lambda}{2} (\text{grad } \rho)^2, \quad (7)$$

where term $(\lambda/2) (\text{grad } \rho)^2$ is added to the volume free energy $\rho \alpha(\rho)$ of a compressible fluid and $\lambda = 2\rho \varepsilon'_\beta(\rho, \beta)$ is assumed to be constant at a given temperature [24]. Specific free energy α enables to connect continuously liquid and vapor bulks and pressure $P(\rho) = \rho^2 \alpha'_\rho(\rho)$ is similar to van der Waals one.

Near a solid wall, London potentials of liquid-liquid and liquid-solid interactions are :

$$\left\{ \begin{array}{l} \varphi_{ll} = -\frac{c_{ll}}{r^6}, \quad \text{when } r > \sigma_l \text{ and } \quad \varphi_{ll} = \infty \text{ when } r \leq \sigma_l, \\ \varphi_{ls} = -\frac{c_{ls}}{r^6}, \quad \text{when } r > \delta \text{ and } \quad \varphi_{ls} = \infty \text{ when } r \leq \delta, \end{array} \right.$$

where c_{ll} and c_{ls} are two positive constants associated with Hamaker constants, σ_l and σ_s denote fluid and solid molecular diameters, $\delta = \frac{1}{2}(\sigma_l + \sigma_s)$ is the minimal distance between centers of fluid and solid molecules. Forces between liquid and solid are short range and can be described simply by adding a special energy at the surface. This energy is the contribution to the solid/fluid

interfacial energy which comes from direct contact. This is not the entire interfacial energy: another contribution comes from the distortions in the density profile near the wall [33,34,38]. For a plane solid wall (at a molecular scale), this surface free energy is in the form :

$$\phi(\rho) = -\gamma_1 \rho + \frac{1}{2} \gamma_2 \rho^2. \quad (8)$$

Here ρ denotes the fluid density value at surface (S); constants γ_1 , γ_2 and λ are positive and given by the mean field approximation :

$$\gamma_1 = \frac{\pi c_{ls}}{12\delta^2 m_l m_s} \rho_{sol}, \quad \gamma_2 = \frac{\pi c_{ll}}{12\delta^2 m_l^2}, \quad \lambda = \frac{2\pi c_{ll}}{3\sigma_l m_l^2}, \quad (9)$$

where m_l and m_s denote respectively masses of fluid and solid molecules, ρ_{sol} is the solid density [34].

We consider a plane liquid layer contiguous to its vapor bulk and in contact with a plane solid wall (S); the z -axis is perpendicular to the solid surface. The liquid film thickness is denoted by h ; the conditions in the vapor bulk are $\text{grad } \rho = 0$ and $\Delta \rho = 0$ with Δ denoting the Laplace operator.

Far below from the critical point of the fluid, a way to compute the total free energy of the complete liquid-vapor layer is to add the surface energy of the solid wall (S) at $z = 0$, the energy of the liquid layer (L) located between $z = 0$ and $z = h$, the energy of the sharp liquid-vapor interface of a few Angström thickness assimilated to a surface (Σ) at $z = h$ and the energy of the vapor layer located between $z = h$ and $z = +\infty$ [42]. The liquid at level $z = h$ is situated at a distance order of two molecular diameters from the vapor bulk and the vapor has a negligible density with respect to the liquid density [43]. In our model, the two last energies can be expressed with writing a unique energy ψ per unit surface located on the mathematical surface (Σ) at $z = h$: by a calculus like in Ref. [34], we can write ψ in the same form than Rel. (8) and also expressed as in Ref. [38] in the form $\psi(\rho) = -\gamma_5 \rho + \frac{1}{2} \gamma_4 \rho^2$; but with a *wall* corresponding to a *negligible density*, $\gamma_5 \simeq 0$, the surface free energy ψ is reduced to :

$$\psi(\rho) = \frac{\gamma_4}{2} \rho^2, \quad (10)$$

where ρ is the liquid density at level $z = h$ and γ_4 is associated with a distance d of the order of the fluid molecular diameter (then $d \simeq \delta$ and $\gamma_4 \simeq \gamma_2$). Consequently, due to the small vapor density, the surface free energy ψ is the same than the surface free energy of a liquid in contact with a vacuum.

Complementary to this argumentation, we will see, in section 4, that the boundary condition at surface (Σ) associated with surface energy (10) yields a density value corresponding to an intermediate density between liquid and vapor and which can be considered as a density value of a dividing-like surface separating liquid and vapor inside the liquid-vapor interface.

Density-functional (6) of the liquid-vapor layer gets the final form :

$$F = \int \int \int_{(L)} \varepsilon \, dv + \int \int_{(S)} \phi \, ds + \int \int_{(\Sigma)} \psi \, ds. \quad (11)$$

4 Equation of equilibrium and boundary conditions of a thin liquid layer contiguous to its vapor bulk and in contact with a vertical plane solid wall

In case of equilibrium, functional (11) is stationary and yields the *equation of equilibrium* and the *boundary conditions* [36,37,43].

4.1 Equation of equilibrium

The equation of equilibrium is :

$$\operatorname{div} \boldsymbol{\sigma} - \rho \operatorname{grad} \Omega = 0,$$

where Ω is the body force potential and $\boldsymbol{\sigma}$ the stress tensor generalization [44,35],

$$\boldsymbol{\sigma} = -p \mathbf{1} - \lambda \operatorname{grad} \rho \otimes \operatorname{grad} \rho,$$

with $p = \rho^2 \varepsilon'_\rho - \rho \operatorname{div} (\lambda \operatorname{grad} \rho)$.

Let us consider an isothermal vertical film of liquid bounded respectively by a flat solid wall and a vapor bulk; then

$$\operatorname{div} \boldsymbol{\sigma} + \rho g \mathbf{i} = 0 \quad (12)$$

in orthogonal system, where \mathbf{i} is the downward direction of coordinate x (the gravity potential is $\Omega = -gx$).

The coordinate z being external and normal to the flat vertical solid wall, spatial density derivatives *are negligible* in directions other than direction of z corresponding to a very strong gradient of density of the liquid normally to the layer and a weak inhomogeneity along the film. In the complete liquid-vapor layer (we call *interlayer*),

$$\boldsymbol{\sigma} = \begin{bmatrix} a_1 & 0 & 0 \\ 0 & a_2 & 0 \\ 0 & 0 & a_3 \end{bmatrix}, \quad \text{with} \quad \begin{cases} a_1 = a_2 = -P + \frac{\lambda}{2} \left(\frac{d\rho}{dz} \right)^2 + \lambda \rho \frac{d^2 \rho}{dz^2} \\ a_3 = -P - \frac{\lambda}{2} \left(\frac{d\rho}{dz} \right)^2 + \lambda \rho \frac{d^2 \rho}{dz^2} \end{cases}$$

and Eq. (12) yields a constant value at level x for the eigenvalue a_3 ,

$$P + \frac{\lambda}{2} \left(\frac{d\rho}{dz} \right)^2 - \lambda \rho \frac{d^2\rho}{dz^2} = P_{v_{bx}},$$

where $P_{v_{bx}}$ denotes the pressure $P(\rho_{v_{bx}})$ in the vapor bulk of density $\rho_{v_{bx}}$ bounding the liquid layer at level x . In the interlayer, eigenvalues a_1, a_2 are not constant but depend on the distance z to the solid wall. In all the fluid, Eq. (12) can also be written [35] :

$$\text{grad } (\mu - \lambda \Delta \rho - g x) = 0, \quad (13)$$

where μ is the chemical potential (at a temperature θ) defined to an unknown additive constant. We note that Eqs. (12-13) are independent of surface energies (8) and (10).

The chemical potential is a function of P (and θ); due to the equation of state for pressure P , the chemical potential can be also expressed as a function of ρ (and θ). We choose as *reference chemical potential* $\mu_o = \mu_o(\rho)$ null for bulks of densities ρ_l and ρ_v of phase equilibrium. Due to Maxwell rule, the volume free energy associated with μ_o is $g_o(\rho) - P_o$ where $P_o = P(\rho_l) = P(\rho_v)$ is the bulk pressure and $g_o(\rho) = \int_{\rho_v}^{\rho} \mu_o(\rho) d\rho$ is null for the liquid and vapor bulks of phase equilibrium. The pressure P is :

$$P(\rho) = \rho \mu_o(\rho) - g_o(\rho) + P_o. \quad (14)$$

Thanks to Eq. (13), we obtain in all the fluid *and not only in the interlayer* :

$$\mu_o(\rho) - \lambda \Delta \rho - g x = \mu_o(\rho_b),$$

where $\mu_o(\rho_b)$ is the chemical potential value of a liquid mother bulk of density ρ_b such that $\mu_o(\rho_b) = \mu_o(\rho_{v_b})$, where ρ_{v_b} is the density of the vapor mother bulk bounding the layer *at level* $x = 0$. This property is due to Eq. (13) which is valid not only in the liquid but also in all the fluid independently of the surface energies in the density-functional (11). Equation (13) is also valid in the sharp liquid-vapor interface.

We must emphasize that $P(\rho_b)$ and $P(\rho_{v_b})$ are unequal as for drop or bubble bulk pressures. Likewise, we define a liquid mother bulk of density ρ_{b_x} at level x such that $\mu_o(\rho_{b_x}) = \mu_o(\rho_{v_{bx}})$ with $P(\rho_{b_x}) \neq P(\rho_{v_{bx}})$; ρ_{b_x} is not a fluid density in the liquid layer but density in the liquid bulk from which the interlayer can extend. Then,

$$\lambda \Delta \rho = \mu_o(\rho) - \mu_o(\rho_{b_x}) \quad \text{with} \quad \mu_o(\rho_{b_x}) = \mu_o(\rho_b) + g x \quad (15)$$

and in the interlayer

$$\lambda \frac{d^2\rho}{dz^2} = \mu_{b_x}(\rho), \quad \text{with} \quad \mu_{b_x}(\rho) = \mu_o(\rho) - \mu_o(\rho_{b_x}) \quad (16)$$

4.2 Boundary conditions

The condition at the solid wall (S) associated with the free surface energy (8) yields [36]:

$$\lambda \left(\frac{d\rho}{dn} \right)_{|S} + \phi'(\rho)_{|S} = 0, \quad (17)$$

where n is the external normal direction to the fluid. Eq. (17) yields :

$$\lambda \left(\frac{d\rho}{dz} \right)_{|z=0} = -\gamma_1 + \gamma_2 \rho_{|z=0}.$$

The condition at the liquid-vapor interface (Σ) associated with the free surface energy (10) yields :

$$\lambda \left(\frac{d\rho}{dz} \right)_{|z=h} = -\gamma_4 \rho_{|z=h}. \quad (18)$$

As we will see in Sects. 5 and 6, Rel. (18) takes into account the density at $z = h$ which is smaller, but of the same order, than liquid density. Due to the numerical values of λ and γ_4 in Sect. 6, the density derivative $\frac{d\rho}{dz}$ is large with respect to the variations of the density in the interlayer and corresponds to the drop of density in the liquid-vapor interface in continuous model. Consequently, Rel. (18) defines the film thickness by introducing a reference point inside the liquid-vapor interface bordering the liquid layer with a convenient density at surface $z = h$ considered as a kind of dividing-like surface in a continuous model for the liquid-vapor interface ([31], Chapter 3).

5 The disjoining pressure for vertical liquid films

Eq. (1) can be extended with the disjoining pressure at level x [16] :

$$\Pi = P_{v_{b_x}} - P_{b_x},$$

where P_{b_x} and $P_{v_{b_x}}$ are the pressures in liquid and vapor mother bulks corresponding to level x . At a given temperature θ , Π is a function of ρ_{b_x} or equivalently a function of x . Let us denote by

$$g_{b_x}(\rho) = g_o(\rho) - g_o(\rho_{b_x}) - \mu_o(\rho_{b_x})(\rho - \rho_{b_x}), \quad (19)$$

the primitive of $\mu_{b_x}(\rho)$ null for ρ_{b_x} . Consequently, from Eq. (14),

$$\Pi(\rho_{b_x}) = -g_{b_x}(\rho_{v_{b_x}}), \quad (20)$$

and an integration of Eq. (16) yields :

$$\frac{\lambda}{2} \left(\frac{d\rho}{dz} \right)^2 = g_{bx}(\rho) + \Pi(\rho_{bx}). \quad (21)$$

The reference chemical potential linearized near ρ_l is $\mu_o(\rho) = \frac{c_l^2}{\rho_l}(\rho - \rho_l)$ where c_l is the isothermal sound velocity in liquid bulk ρ_l at temperature θ [45]. In the liquid part of the liquid-vapor film, Eq. (16) of density profile yields :

$$\lambda \frac{d^2\rho}{dz^2} = \frac{c_l^2}{\rho_l}(\rho - \rho_b) - g x \equiv \frac{c_l^2}{\rho_l}(\rho - \rho_{bx}) \quad \text{with} \quad \rho_{bx} = \rho_b + \frac{\rho_l}{c_l^2} g x. \quad (22)$$

The reference chemical potential linearized near ρ_v is $\mu_o(\rho) = \frac{c_v^2}{\rho_v}(\rho - \rho_v)$ where c_v is the isothermal sound velocity in vapor bulk ρ_v at temperature θ [45]. In the vapor part of the liquid-vapor film,

$$\lambda \frac{d^2\rho}{dz^2} = \frac{c_v^2}{\rho_v}(\rho - \rho_{vb}) - g x \equiv \frac{c_v^2}{\rho_v}(\rho - \rho_{vbx}) \quad \text{with} \quad \rho_{vbx} = \rho_{vb} + \frac{\rho_v}{c_v^2} g x.$$

Due to Eq. (15), $\mu_o(\rho)$ has the same value for ρ_{vbx} and ρ_{bx} , then

$$\frac{c_l^2}{\rho_l}(\rho_{bx} - \rho_l) = \mu_o(\rho_{bx}) = \mu_o(\rho_{vbx}) = \frac{c_v^2}{\rho_v}(\rho_{vbx} - \rho_v), \quad \text{and}$$

$$\rho_{vbx} = \rho_v \left(1 + \frac{c_l^2}{c_v^2} \frac{(\rho_{bx} - \rho_l)}{\rho_l} \right).$$

In the liquid and vapor parts of the interlayer we have,

$$g_o(\rho) = \frac{c_l^2}{2\rho_l}(\rho - \rho_l)^2 \quad (\text{liquid}) \quad \text{and} \quad g_o(\rho) = \frac{c_v^2}{2\rho_v}(\rho - \rho_v)^2 \quad (\text{vapor}).$$

From Eqs (19)-(20) we deduce immediately the disjoining pressure at level x

$$\Pi(\rho_{bx}) = \frac{c_l^2}{2\rho_l}(\rho_l - \rho_{bx}) \left[\rho_l + \rho_{bx} - \rho_v \left(2 + \frac{c_l^2}{c_v^2} \frac{(\rho_{bx} - \rho_l)}{\rho_l} \right) \right]. \quad (23)$$

Due to $\rho_v \left(2 + \frac{c_l^2}{c_v^2} \frac{(\rho_{bx} - \rho_l)}{\rho_l} \right) \ll \rho_l + \rho_{bx}$, we get

$$\Pi(\rho_{bx}) \approx \frac{c_l^2}{2\rho_l}(\rho_l^2 - \rho_{bx}^2).$$

At level $x = 0$, the liquid mother bulk density is closely equal to ρ_l (density of liquid in phase equilibrium) and because of Eq. (22), Π can be considered

as a function of x :

$$\Pi(x) = -\rho_l g x \left(1 + \frac{g x}{2 c_l^2} \right). \quad (24)$$

Now, we consider a film of thickness h_x at level x ; the density profile in the liquid part of the liquid-vapor film is solution of :

$$\left\{ \begin{array}{l} \lambda \frac{d^2 \rho}{dz^2} = \frac{c_l^2}{\rho_l} (\rho - \rho_{b_x}), \\ \text{with } \lambda \frac{d\rho}{dz} \Big|_{z=0} = -\gamma_1 + \gamma_2 \rho|_{z=0} \quad \text{and} \quad \lambda \frac{d\rho}{dz} \Big|_{z=h_x} = -\gamma_4 \rho|_{z=h_x}. \end{array} \right. \quad (25)$$

Quantities τ and d are defined such that :

$$\tau \equiv \frac{1}{d} = \frac{c_l}{\sqrt{\lambda \rho_l}}, \quad (26)$$

where d is a reference length and we introduce coefficient $\gamma_3 \equiv \lambda \tau$. The solution of system (25) is :

$$\rho = \rho_{b_x} + \rho_{1_x} e^{-\tau z} + \rho_{2_x} e^{\tau z}, \quad (27)$$

where the boundary conditions at $z = 0$ and h_x yield the values of ρ_{1_x} and ρ_{2_x} :

$$\left\{ \begin{array}{l} (\gamma_2 + \gamma_3) \rho_{1_x} + (\gamma_2 - \gamma_3) \rho_{2_x} = \gamma_1 - \gamma_2 \rho_{b_x}, \\ -e^{-h_x \tau} (\gamma_3 - \gamma_4) \rho_{1_x} + e^{h_x \tau} (\gamma_3 + \gamma_4) \rho_{2_x} = -\gamma_4 \rho_{b_x}. \end{array} \right.$$

The liquid density profile is a consequence of Eq. (27) when $z \in [0, h_x]$.

By taking Eq. (27) into account in Eq. (21) and $g_{b_x}(\rho)$ in linearized form in the liquid part of the interlayer, we get immediately

$$\Pi(\rho_{b_x}) = -\frac{2 c_l^2}{\rho_l} \rho_{1_x} \rho_{2_x},$$

and consequently,

$$\begin{aligned} \Pi(\rho_{b_x}) = & \frac{2 c_l^2}{\rho_l} \left[(\gamma_1 - \gamma_2 \rho_{b_x})(\gamma_3 + \gamma_4) e^{h_x \tau} + (\gamma_2 - \gamma_3) \gamma_4 \rho_{b_x} \right] \times \\ & \frac{\left[(\gamma_2 + \gamma_3) \gamma_4 \rho_{b_x} - (\gamma_1 - \gamma_2 \rho_{b_x})(\gamma_3 - \gamma_4) e^{-h_x \tau} \right]}{\left[(\gamma_2 + \gamma_3)(\gamma_3 + \gamma_4) e^{h_x \tau} + (\gamma_3 - \gamma_4)(\gamma_2 - \gamma_3) e^{-h_x \tau} \right]^2}. \end{aligned} \quad (28)$$

By identification of expressions (23) and (28), we get a relation between h_x and ρ_{b_x} and consequently a relation between disjoining pressure $\Pi(\rho_{b_x})$ and thickness h_x of the liquid film. For the sake of simplicity, we denote finally the disjoining pressure by $\Pi(h_x)$ which is a function of h_x at temperature θ .

Due to the fact that $\rho_{b_x} \simeq \rho_b \simeq \rho_l$ [16], the disjoining pressure reduces to the simplified expression :

$$\Pi(h_x) = \frac{2c_l^2}{\rho_l} \left[(\gamma_1 - \gamma_2\rho_l)(\gamma_3 + \gamma_4)e^{h_x\tau} + (\gamma_2 - \gamma_3)\gamma_4\rho_l \right] \times \frac{\left[(\gamma_2 + \gamma_3)\gamma_4\rho_l - (\gamma_1 - \gamma_2\rho_l)(\gamma_3 - \gamma_4)e^{-h_x\tau} \right]}{\left[(\gamma_2 + \gamma_3)(\gamma_3 + \gamma_4)e^{h_x\tau} + (\gamma_3 - \gamma_4)(\gamma_2 - \gamma_3)e^{-h_x\tau} \right]^2}. \quad (29)$$

Let us notice an important property of a mixture of a van der Waals fluid and a perfect gas where the total pressure is the sum of the partial pressures of components [45]: at equilibrium, the partial pressure of the perfect gas is constant through the liquid-vapor-gas layer -where the perfect gas is dissolved in the liquid. The disjoining pressure of the mixture is the same than for a single van der Waals fluid and calculations and results are identical to those previously obtained.

6 Numerical calculations for water wetting a vertical plane wall

Our aim is not to propose an exhaustive study of the disjoining pressure of water for all physicochemical conditions associated with different walls but to point out examples such that previous results provide new values of maximum height for a vertical water film damping a plane wall.

Calculations are made with *Mathematica*TM. The disjoining pressure Π and the Gibbs free energy G are presented as functions of h_x . The h_x values must be greater than the molecular radius of water corresponding to the smallest thickness of the liquid layer.

The graphs of $\Pi(h_x)$ are directly issued from Rel. (29) with different physical values obtained in the literature. The graphs of $G(h_x)$ are deduced from Rel. (3). As a function of h_x , function $\Pi(h_x)$ is not an analytically integrable expression; consequently G -graphs are computed by *Mathematica*TM but with help of a numerical process.

For a few nanometer range, the film thickness is not exactly h_x ; at this range we must add to h_x the liquid part of the liquid-vapor interface bordering the liquid layer (the thickness of which is neglected for films of several nanometers). We can estimate this part thickness at $2\sigma_l$ (half of the thickness of water liquid-vapor interface at 20° Celsius [24,31]). The film thickness is $e_x \approx h_x + 2\sigma_l$. The previous results in sections 3-5 remain unchanged by using h_x in place of the liquid thickness h .

When $h_x = 0$ (corresponding to the dry wall), the value of G is the spreading coefficient S (see Fig. 2). We must emphasize that point P associated with the pancake layer is observed, on the numerical curves, to be closely an inflexion point of graph $\Pi(h)$ corresponding to the strongest stability of films (maximum of $\partial^2 G / \partial h^2$) [38,39]. To obtain the pancake thickness corresponding to the

smallest film thickness, we draw the graphs of $\Pi(h_x)$ and $G(h_x)$, when $h_x \in [\frac{1}{2}\sigma_l, \ell]$, where ℓ is a distance of few tens of Angström.

At $\theta = 20^\circ$ Celsius, we consider successively water wetting a wall in silicon as a reference of material and water damping a less wetting wall.

In c.g.s. units

The experimental estimates of coefficients are obtained in Refs. [17] and [46] :

$$\begin{aligned}\rho_l &= 0.998, \\ c_l &= 1.478 \times 10^5, \\ c_{ll} &= 1.4 \times 10^{-58}, \\ \sigma_l &= 2.8 \times 10^{-8} \text{ (2.8 Angström or 0.28 nanometer)}, \\ m_l &= 2.99 \times 10^{-23} .\end{aligned}$$

From Rel. (9), we deduce

$$\begin{aligned}\lambda &= 1.17 \times 10^{-5}, \\ \gamma_2 &= \gamma_4 = 54.2 .\end{aligned}$$

From $\gamma_3 = \lambda\tau$ and Rel. (26), we get

$$\begin{aligned}\gamma_3 &= 506, \\ d &= 2.31 \times 10^{-8} .\end{aligned}$$

We consider two cases :

a) For silicon (as a reference of wall damped by water), physical characteristics are,

$$\begin{aligned}\sigma_s &= 2.7 \times 10^{-8}, \\ m_s &= 4.65 \times 10^{-23}, \\ \rho_{sol} &= 2.33 .\end{aligned}$$

No information is available for water-silicon interactions; if we assume that

$$\begin{aligned}c_{ll} &= c_{ls} = 1.4 \times 10^{-58}, \text{ we deduce} \\ \gamma_1 &= 81.2 .\end{aligned}$$

b) We consider a material such that $\gamma_1 = 75$ (the material is less damped by liquid water). The other values of the coefficients of the material are assumed to be the same than in case *a*). We will see that these values are well adapted to our problem.

Corresponding to Rel. (4), the graphs of $\Pi(h_x)$ in cases *a*) and *b*) are easy to plot following the liquid layer thickness for stable and unstable domains. The G -graphs are deduced by numerical integration following the bound h_x ; the limit $+\infty$ is replaced by ten thousand molecular diameters of water molecules. Due to $h_x > \frac{1}{2}\sigma_l$, it is not possible to obtain numerically the limit point W corresponding to the dry wall (Fig. 2). This point is graphically obtained by an interpolation associated with the concave part of the G -curve. Point P follows from the drawing of the tangent line from W to the G -curve.

It is important to point out that reference length d is of the same order than σ_l , σ_s and δ and seems a good length order for very thin films.

In Fig. 3, we present disjoining pressure graphs in the two cases. Real parts of disjoining pressure graphs corresponding to $\partial\Pi/\partial h_x < 0$ are plain lines of the curves and are associated with thickness liquid layers of several molecules. Dashed lines of the curves have no real existence.

From reporting the pancake thickness of the h_x axis for the Π -curve, we deduce its disjoining pressure corresponding value; the maximum of altitude of topmost trees is calculated with Eq. (24).

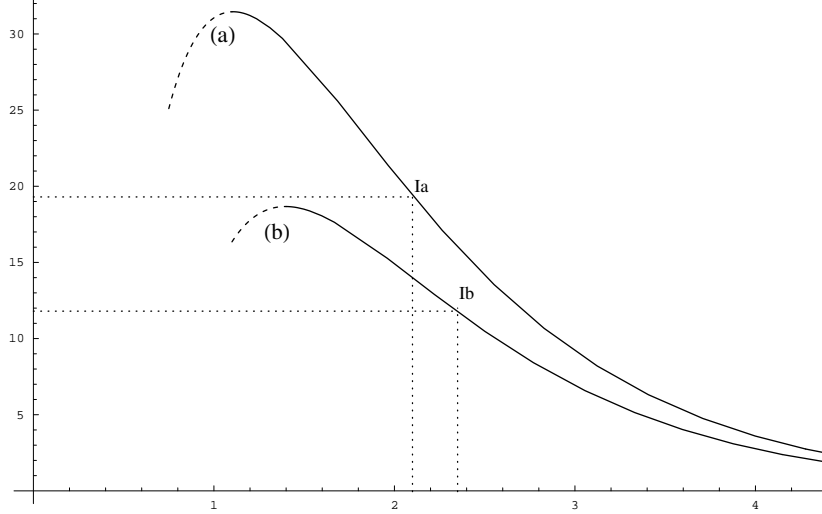


Fig. 3. Graphs represent the disjoining pressure as a function of the liquid layer thickness h_x for liquid water at 20°C in contact with different walls (the total thickness of the film is $e_x \approx h_x + 2\sigma_l$). The unit of x -axis is $d = 2.31 \times 10^{-8}\text{ cm}$; the unit of y -axis is one atmosphere. Curve (a) corresponds to water wetting a silicon wall ($\gamma_1 = 81.2\text{ cgs}$); curve (b) corresponds to water wetting a less damped wall ($\gamma_1 = 75\text{ cgs}$). Points Ia and Ib are the inflexion points of curves (a) and (b) corresponding roughly to points P in Fig. 4.

In Fig. 4, we present graphs of the Gibbs free energy G as a function of h_x . The limit of the film thickness is associated to the *pancake* thickness $e_p \approx h_p + 2\sigma_l$ when the liquid film coexists with the dry wall. The spreading coefficient values are associated with point P : at point P , which is numerically close to the inflexion point of $\Pi(h_x)$, the tangent goes to point W of the y -axis (where $G(0) = S$). In the two cases, the total pancake thickness $e_p = h_p + 2\sigma_l$ is of one nanometer order corresponding to a good thickness value for a high-energy surface [39].

From the graphs, we deduce $S \approx 64\text{ cgs}$ in case a) and $S \approx 40\text{ cgs}$ in case b) corresponding to a less energetic wall. However, crude sap is not pure water. Its liquid-vapor surface tension has a lower value than surface tension of pure water (72 cgs at 20°C) and it is possible to obtain the same spreading coefficients with less energetic surfaces.

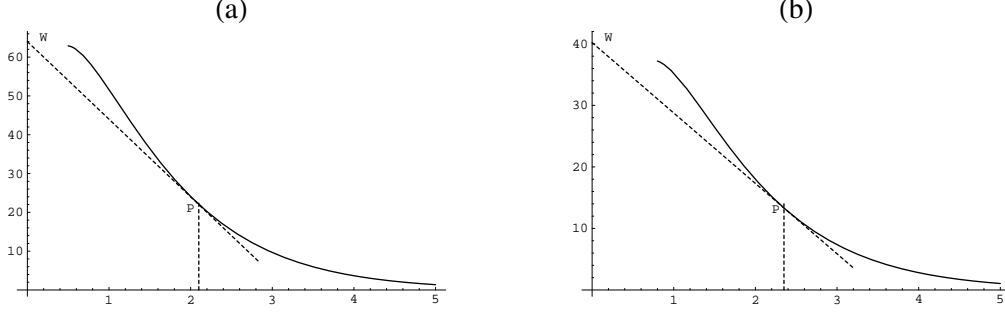


Fig. 4. Graphs represent the film Gibbs free energy per unit area as a function of the liquid layer thickness for liquid water at 20° C in contact with two different walls. The unit of x -axis is $d = 2.31 \times 10^{-8} \text{ cm}$; the unit of y -axis is one *cgs* unit of superficial tension. Graph (a) corresponds to water wetting a silicon wall ($\gamma_1 = 81.2 \text{ cgs}$); graph (b) corresponds to water wetting a less damped wall ($\gamma_1 = 75 \text{ cgs}$). Point W is associated with the surface energy of the dry wall and point P is associated with h_p corresponding to the pancake layer where the film coexists with the dry wall; the smallest film thickness possible is $e_p \approx h_p + 2\sigma_l$.

When $|x|$ is of some hundred meters, Eq. (24) yields :

$$\Pi(x) \simeq \rho_l g x.$$

The maximum of altitude $|x_M|$ corresponds to the pancake layer. We add 20 meters to this altitude, corresponding to the ascent of sap due to hydrodynamic, capillarity and osmotic pressure. In case *b*), the material has a lower surface energy than silicon and we obtain a film height of 140 meters.

7 Conclusion

In this article, we considered a very thin liquid film damping and rising along a vertical plane wall as a model of the ascent of sap in xylem tubes.

At its bottom, the film is bordered on a liquid meniscus corresponding to a xylem tube filled with sap up to an altitude of a few ten meters. Above this altitude, the xylem tube is embolized such as the liquid water thin film wets the wall of the tube.

The study is static. The motor of the sap motion is induced by the transpiration across micropores located in tree leaves [3] and is studied by lubrication approximation in a model adapted to thin layers [20,47]. It is natural to forecast that the diameters of xylem tubes must be the result of a competition between evaporation in tubes which reduces the flow of sap and the flux of transpiration in micropores inducing the motion strength.

Computational methods, such as density-functional theory (DFT) and kinetic Monte Carlo (KMC) have already had major success in nanoscience. We have

obtained the disjoining pressure and Gibbs energy curves for two different solid walls. In cases of Lifshitz analysis [18] and van der Waals theory [30], the disjoining pressure behaviors are respectively as $\Pi \sim h^{-3}$ and $\Pi \sim \exp(-h)$. These two behaviors seem unable to study a film with a thickness between one and three nanometers.

It is wondering to observe that the density-functional theory expressed by a rough model correcting van der Waals' with a surface density-functional at the walls enables to obtain a good order of magnitude of the ascent of sap. This result is obtained without any complex weighted density-functional and without taking into account the quantum effects corresponding to less than an Ångström length scale. The surface density-functional at the wall takes into account a power-law behavior associated with a balance between attractive and repulsive forces, the square-gradient functional schematizing the liquid-vapor interface effects. This biophysical observation seems to prove that this kind of functional can be a good tool to study models of liquids in contact with solids at a small nanoscale range.

Due to a remark by James R. Henderson [48], it is interesting to note that *if we switch the micro-tube surfaces to wedge geometry as in [49] or to corrugated surface then, it is much easier to obtain the complete wetting requirement. Thus, plants can avoid having very high energy surfaces, but still be internally wet, if they pass liquids through wedge shaped corrugated pores. The wedge does not have to be perfect on the nanometer scale to significantly enhance the amount of liquid that would be passed at modest pressures corresponding to nano-sized planar films. It is bound to improve on the calculation because it enhances the surface to volume ratio.*

In such a case, we remark that the wall boundary can always be considered as a plane surface with an average surface energy as in Wenzel's formula [50].

Acknowledgment: The author dedicates the paper to the memory of Professor Pierre Casal, his Master and friend.

References

- [1] Flindt R.: Amazing Numbers in Biology, Springer, Berlin (2006).
- [2] Koch W., Sillett S.C., Jennings G.M., Davis S.D.: The limit to tree height, Nature **428**, 851-854 (2004).
- [3] Zimmermann M.H.: Xylem Structure and the Ascent of Sap, Springer, Berlin (1983).
- [4] Dixon H.H., Joly J.: On the ascent of sap, Phil. Trans. Roy. Soc. London, B **186**, 563-576 (1894).

- [5] van der Honert T.H.: Water transport in plants as a catenary process, Discussions of the Faraday Society **3**, 1105-1113 (1948).
- [6] Tyree M.T., Sperry J.S.: The vulnerability of xylem to cavitation and embolism, Annu. Rev. Plant Physiol. Plant Mol. Biol. **40**, 19-38 (1989).
- [7] Zimmermann U., Schneider H., Wegner L.H., Haase A.: Water ascent in tall trees: does evolution of land plants rely on a highly metastable state? Tansley review, New Phytologist **162**, 575-615 (2004).
- [8] Preston R.D.: Movement of water in higher plants. In: Deformation and Flow in Biological Systems, Ed. Frey-Wyssling A, North Holland Publishing, Amsterdam, 257-321 (1952).
- [9] Mackay J.F.G., Weatherley P.E.: The effects of transverse cuts through the stems of transpiring woody plants on water transport and stress in the leaves, J. of Exp. Botany **24**, 15-28 (1973).
- [10] Eisenhut G.: Neue Erkenntnisse ber den Wassertransport in Bumen, HolzZentralblatt **55**, 851-853 (1988).
- [11] Benkert R, Balling A, Zimmermann U.: Direct measurements of the pressure and flow in the xylem vessels of nicotiana tabacum and their dependence on flow resistance and transpiration rate, Botanica Acta **104**, 423-432 (1991).
- [12] Balling A., Zimmermann U.: Comparative measurements of the xylem pressure of nicotiana plants by means of the pressure bomb and pressure probe, Planta **182**, 325-338 (1990).
- [13] Zimmermann U., Haase A., Langbein D., Meinzer F.: Mechanism of long-distance water transport in plants: a re-examination of some paradigms in the light of new evidence, Phil. Trans. Roy. Soc. London **431**, 19-31 (1993).
- [14] Tyree M.T.: The cohesion-tension theory of sap ascent: current contreversies, J. Exp. Botany, **48**, 1753-1765 (1997).
- [15] dell'Isola F., Gouin H., Rotoli G., Nucleation of spherical shell-like interfaces by second gradient theory: numerical simulations, Eur. J. Mech., B/Fluids, **15**, 4, pp. 545-568 (1996).
- [16] Derjaguin B.V., Chuarev N.V., Muller V.M.: Surfaces Forces, Plenum Press, New York (1987).
- [17] Israelachvili J.: Intermolecular Forces, Academic Press, New York (1992).
- [18] Dzyaloshinsky I.E., Lifshitz E.M., Pitaevsky L.P.: The general theory of van der Waals forces, Adv. Phys., **10**, 165-209 (1961).
- [19] Ono S., Kondo S., Molecular theory of surface tension in liquid. In: Structure of Liquids, S. Flügge (ed.) Encyclopedia of Physics, X, Springer verlag, Berlin (1960).
- [20] Gouin H., Gavriluk S.: arXiv:0809.3489, Dynamics of liquid nanofilms, Int. J. Eng. Sci. (2008) doi: 10.1016/j.engsci 2008.05.002 (in press).

- [21] Bhushan B.: Springer Handbook of Nanotechnology, Springer, Berlin, (2004).
- [22] van der Waals J.D.: Thermodynamique de la capillarité dans l'hypothèse d'une variation continue de densité, Archives Néerlandaises **28**, 121-209 (1894-1895).
- [23] Widom B.: What do we know that van der Waals did not know?, Physica A **263**, 500-515 (1999).
- [24] Rocard Y.: Thermodynamique, Masson, Paris (1952).
- [25] Chernov A.A., Mikheev L.V.: Wetting of solid surfaces by a structured simple liquid: Effect of fluctuations, Phys. Rev. Lett. **60**, 2488 - 2491 (1988).
- [26] Chernov A.A., Mikheev L.V.: Wetting and surface melting: Capillary fluctuations versus layerwise short-range order, Physica A **157**, 1042-1058 (1989).
- [27] Evans R.: The nature of liquid-vapour interface and other topics in the statistical mechanics of non-uniform classical fluids, Adv. Phys. **28**, 143-200 (1979).
- [28] Evans R., Leote de Carvalho J.F., Henderson J.R., Hoyle D.C.: Asymptotic decay of correlations in liquids and their mixtures, J. Chem. Phys. **100**, 591-603 (1994)
- [29] Fisher M.E., Jin A.J.: Effective potentials, constraints, and critical wetting theory, Phys. Rev. B **44**, 3, 1430 - 1433 (1991).
- [30] Henderson J.R.: Statistical mechanics of the disjoining pressure of a planar film, Phys. Rev. E **72**, 051602 (2005).
- [31] Rowlinson J.S., Widom B.: Molecular Theory of Capillarity, Clarendon Press, Oxford (1984).
- [32] Nakanishi H., Fisher M.E., Multicriticality of wetting, prewetting, and surface transitions, Phys. Rev. Lett. **49**, 1565 - 1568 (1982).
- [33] Cahn J.W.: Critical point wetting, J. Chem. Phys. **66**, 3667-3672 (1977).
- [34] Gouin H.: arXiv:0801.4481, Energy of interaction between solid surfaces and liquids, J. Phys. Chem. B **102**, 1212-1218 (1998).
- [35] Gouin H.: Utilization of the second gradient theory in continuum mechanics to study the motion and thermodynamics of liquid-vapor interfaces, Physicochemical Hydrodynamics, B Physics **174**, 667-682 (1987).
- [36] Gouin H., Kosiński W.: arXiv:0802.1995, Boundary conditions for a capillary fluid in contact with a wall, Arch. Mech. **50**, 907-916 (1998).
- [37] Seppecher P.: Equilibrium of a Cahn and Hilliard fluid on a wall: influence of the wetting properties of the fluid upon stability of a thin liquid film, Eur. J. Mech., B/fluids **12**, 61-84 (1993).
- [38] de Gennes P.G.: Wetting : statics and dynamics, Rev. Mod. Phys. **57**, 827-863 (1985).

- [39] de Gennes P.G., Brochard-Wyart F., Quéré D.: *Capillarity and Wetting Phenomena: Drops, Bubbles, Pearls, Waves*, Springer, New York (2004).
- [40] Sheludko A.: Thin liquid films, *Adv. Colloid Interface Sci.* **1**, 391-464 (1967).
- [41] Lutsko J.M.: Density functional theory of inhomogeneous liquids. I. The liquid-vapor interface in Lennard-Jones fluids, *J. Chem. Phys.* **127**, 054701 (2007).
- [42] Gavriluk S.L., Akhatov I.: Model of a liquid nanofilm on a solid substrate based on the van der Waals concept of capillarity, *Phys. Rev. E.* **73**, 021604 (2006).
- [43] Pismen L.M., Pomeau Y.: Disjoining potential and spreading of thin liquid layers in the diffuse-interface model coupled to hydrodynamics, *Phys. Rev. E.* **62**, 2480-2492 (2000).
- [44] Truskinovsky L.: Equilibrium phase boundaries, *Sov. Phys. Dokl.* **27**, 551-553 (1982).
- [45] Gouin H., Espanet L.: arXiv:0807.5023, Bubble number in a cavitating flow, *Comptes Rendus Acad. Sci. Paris* **328**, IIb 151-157 (2000).
- [46] *Handbook of Chemistry and Physics*, 65th Edition, CRC Press, Boca Raton (1984-1985).
- [47] Gouin H.: arXiv:0809.2346, A mechanical model for liquid nanolayers, in: *Waves and Stability in Continuous Media*, Eds. N. Manganaro, R. Monaco & S. Rionero, World Scientific, Singapore, 306-315 (2008).
- [48] Henderson J.R.: Private communication and discussion (September 2008).
- [49] Concus P., Finn R.: On the behavior of a capillary surface in a wedge, *Proc. Nat. Acad. Sci.* **63**, 292-299 (1969).
- [50] Wenzel T.N.: Surface roughness and contact angle. *J. Phys. Colloid. Chem.* **53**, 1466 (1949).